# Modeling of Solid-State Polycondensation. II. Reactor Design Issues

**FREDERICK K. MALLON, W. HARMON RAY**

Department of Chemical Engineering, University of Wisconsin, Madison, Wisconsin 53706

*Received 7 July 1997; accepted 9 September 1997*

**ABSTRACT:** The relative merits of the moving packed bed, fluidized bed, and stirred bed reactors for solid-state polycondensation are discussed along with methods for improving these designs. A general model to describe continuous solid-state polymerization reactors is then developed and illustrated by a case study of a moving packed bed reactor showing the relative importance of operating variables. The model also predicts the dynamic behavior in response to several process inputs. © 1998 John Wiley & Sons, Inc. J Appl Polym Sci 69: 1775–1788, 1998

**Key words:** polymer reactor engineering; PET; reactor modeling

## INTRODUCTION

The widespread application of PET (polyethylene terephthalate) in the automotive tire cord and soft drink bottle markets has led to multibillion dollar markets for resin that is best produced in the solid state. Although there has been extensive published modeling work on melt reactors for PET and nylon, there seems to be none for solid-state reactors.

The principal polycondensation chain building reaction is of the form

$$P_m + P_n \leftrightarrow P_{m+n} + C \qquad (1)$$

where $C$ is a condensate such as ethylene glycol or water. The finite equilibrium constant for eq. (1) means that, to achieve high molecular weights, the condensate molecule must be removed to drive the equilibrium towards the higher molecular weights. The condensate removal is often diffusion limited in solid-state polymerization, even for small polymer particles (cf. part I of this series[1]). Furthermore, in a solid-state reactor, the removal rate of condensate is affected by the time and spatial variation in gas phase temperature and condensate concentration because these lead to variations in the driving force for gas–solid heat and mass transfer.

In part I of this study, a solid-state polymerization model for single polymer particles was developed using the ideas from many previous authors, particularly Ravindranath et al.[2] The new features of this particle model were (1) crystallization induced fractionation[3] and its effect on reaction kinetics and equilibrium; (2) dynamic variation of the degree of crystallinity and its effect on mass transport in the polymer; (3) a more comprehensive kinetic scheme; and (4) more detailed modeling of gas–solid mass transfer.

Usual industrial practice for the solid-state polymerization of PET consists of first polymerizing the material in the melt to a molecular weight normally between 10,000 and 20,000. The melt is extruded and formed into solid particles with a diameter of about 2 mm. These particles are then fed to a solid-state polymerizer that is often a moving packed bed reactor, a diagram of which is in Figure 1. The particles move downward in the reactor and a countercurrent purge gas carries off the desorbed condensate to drive the reaction to

*Correspondence to:* W. H. Ray.

Journal of Applied Polymer Science, Vol. 69, 1775–1788 (1998)
 CCC 0021-8995/98/091775-14

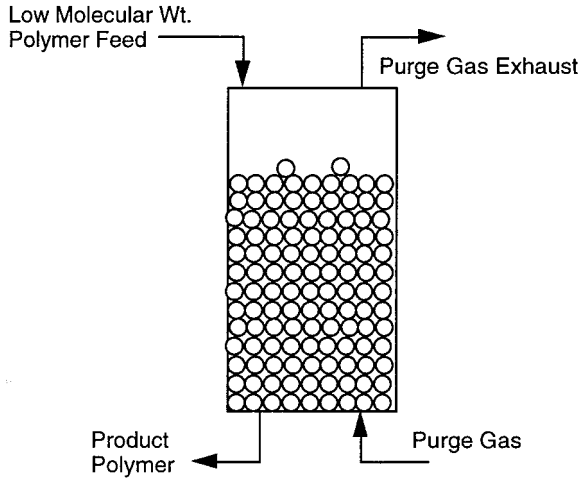


**Figure 1** Schematic of a moving packed bed reactor.

high molecular weights. Other reactors that are employed include fluidized bed and stirred bed reactors. The model developed in this work allows both dynamic and steady-state simulation of particle and reactor scale phenomena in many types of solid-state reactors.

Yau and Cherry[4] recently showed that increasing the concentration of condensates in the inlet purge gas can have a large effect on the formation of gels (very high molecular weight materials) in the polymer. Yau and Cherry explained the suppression of gels by arguing that the enhanced concentrations of water and ethylene glycol lead to reverse reactions, which allow the polymer to relax highly entangled chains. Failing to relax the entangled chains then leads to gels in the cast polymer. The model developed here will explain the experimental results of Yau and Cherry somewhat differently.

## SOME ALTERNATIVE DESIGNS FOR SOLID-STATE REACTORS

There are a variety of possible reactor designs for carrying out solid-state polycondensation on an industrial scale. The most common design at present is a moving packed bed reactor; however, fluidized bed reactors and stirred bed reactors have also been used. Here we shall discuss some of the more important features of several alternative designs.

### Moving Packed Bed Reactors

The recent patent of Yau and Cherry[4] provides some typical operating conditions (at least on the experimental level) for moving packed bed reactors. Yau and Cherry introduce low molecular weight PET chips at the top of a reactor (height 11 ft., diameter 1 ft.). These polymer chips flow by gravity in a quasiplug flow manner towards the bottom (residence time about 40 h). A purge gas (superficial velocity between 2 and 8 cm/s) is introduced at the bottom to carry away the low molecular weight condensates and shift the overall equilibrium to higher molecular weights. These conditions imply a flow rate of about 3400 L of purge gas/kg PET product; however, due to recycling of purge gas, the real fresh feed rate of purge gas is probably lower.

Figure 1 ignores an important characteristic of industrial solid-state polymerization of PET. Producers of PET are known to use purge gas that contains residual ethylene glycol and water. This addition of water and ethylene glycol seems counterproductive, given that the purpose of the purge gas is to remove the ethylene glycol and water [the condensates of eq. (1)]. However, there are two justifications. First, by requiring less of a pure purge, operating costs are reduced. Second, the manufacturer has the aim of producing a highly uniform product. Examining molecular weight particularly, if a certain operation style leads to some particles of low molecular weight and others with high molecular weight, then purchasers of the resin may observe inconsistent operation in their processing steps. The reactor operation described above ignores some of the operating nonidealities and their associated effects on the reaction (Table I). Any one of these factors can cause the produced resin to be heterogeneous. By introducing a purge gas with a small amount of condensate, the overall driving force for mass transfer is reduced. Because areas of high molecular weight will be inhibited from further polymerization while areas of low molecular weight will still be able to polymerize, the effect of the reactor inhomogenieties in Table I is reduced. This resolves all but the last aspect of Table I; the temperature variations still cause variations in the gas–solid mass transfer of condensate. Minimizing heat conduction at the wall helps protect against this operating problem.

### Fluidized Bed Reactor

The common component in Table I is the uneven distribution of some important process variables.

**Table I Effect of Operating Problems in a Moving Packed Bed Reactor**

| Operating Problem | Effect on Polymerization |
|---|---|
| Uneven flow of polymer particles | Different residence times yield different molecular weights |
| Uneven flow of purge gas | Different mass transfer rates yield different molecular weights |
| Uneven radial temperature distribution across the reactor | Different particle reaction/diffusion rates and gas–solid mass transfer rates lead to different molecular weights |

This has led to the proposal of using a fluidized bed instead of a moving packed bed. Such a reactor would be similar to a fluidized bed crystallizer that has been proposed for PET.[5–7] The advantage of the fluidized bed is that the polymer particles would be in a spatially uniform environment and it is somewhat easier to maintain very low condensate concentrations in the purge gas.

The use of a fluidized bed reactor creates other, more difficult, problems, however. Although now all particles experience the same environment, a residence time distribution equivalent to a stirred tank reactor is generated. In other words, the uneven flow of polymer particles (first line of Table I) is traded for the very broad distribution of a stirred tank reactor. This would result in a very broad molecular weight distribution under kinetically controlled conditions. However, by setting the purge gas condensate level at the equilibrium value for the desired final molecular weight, the effects of the residence time distribution would be mitigated somewhat.

One could overcome the residence time distribution problem by linking two to four fluidized beds in series with the possibility of different purge gas condensate concentrations and temperature in each reactor. This would allow high productivity with close control of polymer properties at each stage.

Another alternative would be to operate the fluidized bed in a batch mode with very low purge gas condensate levels. Then the reaction could be carried out very rapidly under kinetic control, as shown in Figure 2. With a battery of such batch fluidized beds in parallel, the upstream and downstream part of the operation could still be continuous.

All modes of fluidized bed operation would require about 100 times the gas flow of the moving packed bed. This larger gas recycle stream would require a larger recycle gas compressor and condensate removal system.

### Stirred Bed Reactor

A stirred bed reactor is another alternative design. A series of vertical or horizontal stirred bed reactors could be used. Reactors with a controlled level of dispersion similar to the AMOCO/CHISSO[8] design (equivalent to four CSTRs in series) would require much lower gas flow rates than the fluidized bed. This design would also reduce dispersion, thus, effectively dealing with all the limitations expressed in Table I. One drawback is the cost of internals. A stirrer operating in a reactor with a residence time of about 20 h could consume significant energy.

Comparison of the detailed capital and operating costs as well as operating details would be necessary to determine the best design alternative for a particular product.

## SOLID-STATE REACTOR MODELING

To understand in detail the features of alternative designs, a fundamental process model is required. In this section, we develop the equations for such a model and, in the next section, we use it to analyze the behavior of a moving packed bed reactor. This section consists of three basic parts: development of the differential equations for modeling

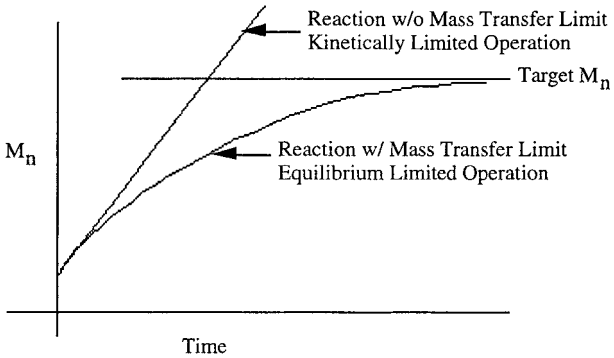


**Figure 2** Decrease in reaction time by avoiding mass transfer limit for solid-state reaction.

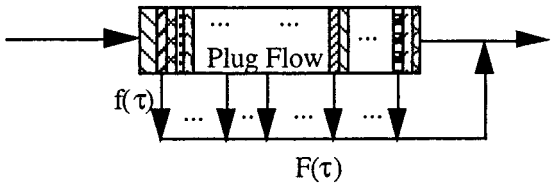


**Figure 3** Segregated flow model of Zwietering.[9]

the polymer phase, development of the differential equations for modeling the reactor gas phase, and development of modeling equations for the energy balance.

## Segregated Chemical Reactor

Because the polymer particles do not coalesce and redisperse, the particle phase in these reactors may be considered as perfectly segregated. On the other hand, the residence time distribution of the polymer particles can be that of a stirred tank, a plug flow reactor, or somewhere intermediate. Segregated reactors with an arbitrary residence time distribution can be understood from the classical work of Zwietering[9] (Fig. 3). In Figure 3, the material moves through the plug flow tubular reactor in a completely segregated fashion while the draw streams are adjusted to create the desired residence time distribution. In this way, any residence time distribution (cf. examples in Fig. 4) can be matched.

The concentration of a tracer, $c(z)$, in the reactor of Figure 3 can be written as

$$\frac{\partial c}{\partial t} = -\frac{\partial (vc)}{\partial z} - F_{\text{exit}}(z)c \qquad (2)$$

where $z$ is the distance along the tube, $v(z)$ is the varying flow rate in the tube, and $F_{\text{exit}}(z)$ is the side draw rate at position $z$. However, by assuming the fluid is incompressible with constant density, a total material balance over all species yields the relation

$$0 = -\frac{\partial v}{\partial z} - F_{\text{exit}}(z) \qquad (3)$$

Therefore, by combining eqs. (2) and (3) and defining reactor residence time by $d\tau = dz/v$ and

$$\tau = \int_0^z \frac{dz'}{v(z')}$$

eq. (2) can be written in terms of the residence time.

$$\frac{\partial c}{\partial t} = -\frac{\partial c}{\partial \tau} \qquad (4)$$

Discretizing eq. (4) and using backwards differences, the following equation is developed

$$\frac{\partial c_k}{\partial t} = \frac{c_{k-1} - c_k}{\Delta \tau_k} \quad k = 1, 2, \cdots N \qquad (5)$$

where $N$ is the number of discretization points and $\Delta\tau_k$ is the discretization step size. Examination of eq. (5) shows that this is just the equation for a series of stirred tanks where $\Delta\tau_k$ is selected as the tank residence time and $c_k$ is the concentration in the tank. Therefore, modeling of the reactor shown in Figure 3 can be carried out with either the mathematical formalism of eq. (2) or with approximation by a series of CSTRs (called "stages" in this work). Modeling with a series of CSTRs includes the same approximation made in writing eq. (5), and introduces some backmixing in what should be perfect flow segregation. Decreasing $\Delta\tau_k$ (i.e., increasing the number of CSTRs) will obviously improve this approximation. The CSTRs-in-series approximation to Figure 3 is shown in Figure 5.

In Figure 3, with an infinite set of draw points, each draw point takes a fraction $f(\tau)$ of the total

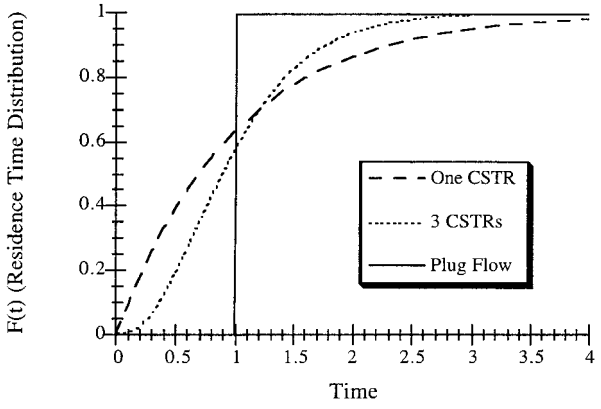


**Figure 4** Residence time distributions.

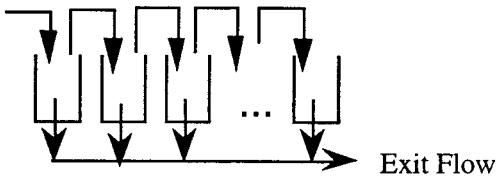


**Figure 5** Approximate segregated flow CSTRS-in-series model.

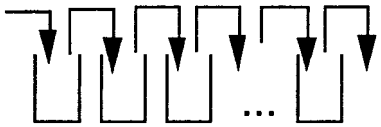

**Figure 6** CSTRs-in-series tubular reactor model.

material entering the reactor, where $f(\tau)$ is the residence time density function and

$$F(\tau) = \int_0^\tau f(\tau')\, d\tau'$$

is the residence time distribution function.

For a CSTR, the functions $f(\tau)$ and $F(\tau)$ are well known to be

$$f(\tau) = \frac{1}{\bar{\tau}} e^{-\tau/\bar{\tau}},\ \mathrm{F}(\tau) = 1 - \exp(-\tau/\bar{\tau}) \quad (6)$$

where $\bar{\tau}$ is the mean residence time. This residence time distribution results when the side draw $f(\tau)$ (Fig. 3) is proportional to the amount of mass in the reactor at residence time, $\tau$, i.e.,

$$f(\tau) = K(1 - F(\tau)) = Ke^{-\tau/\bar{\tau}}$$

The constant $K = 1/\bar{\tau}$ is found from the condition that as $\tau \to \infty$, all material must have left the reactor

$$\left(\int_0^\infty f(\tau)\, d\tau = 1\right)$$

In summary, the key condition for a CSTR residence time distribution is that the withdrawal rate is proportional to the amount remaining in the reactor.

Now, for the approximate model of Figure 5, the drawstreams must be determined in order match the desired residence time distribution. In general, the set of residence time distributions for each tank forms a basis that can be used to fit an arbitrary residence time distribution. We demonstrated above that, to model a stirred tank, the sidestream for each stage must be proportional to the material remaining. For the plug flow tubular reactor, all side streams will be zero, and one obtains the standard CSTRs-in-series result shown in Figure 6. Other reactors can be represented by arbitrary sidedraws to produce the proper residence time distribution.

Having configured the reactor to produce the desired residence time distribution with adequate approximation of segregation, these equations can then be used for all species in the reactor. In addition, diffusion of volatile species within particles is encountered at each position in the reactor.

In the text that follows, stage will refer to the CSTR associated with replacing eq. (2). Collocation point will refer to a radial particle collocation point, and element will refer to a collocation point–stage pair. This may be seen in Figure 7.

The model for a polymer particle contains several collocation points each representing a certain amount of mass. As flow convects $N$ particles from one stage to the next, the flow for each element is proportional to the mass for that element because, for the CSTRs-in-series representation of segregation, the probability of a particle leaving

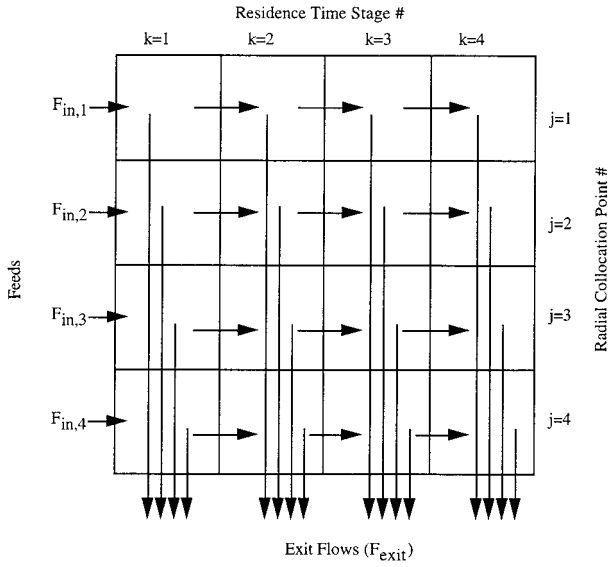


**Figure 7** Modeled flows in a CSTRs-in-series model.

each stage is proportional to the mass at that stage.

$$F_{j,k\rightarrow k+1} \propto M_{j,k} \tag{7}$$

In modeling single particles, eqs. (8) and (9) [numbered eqs. (9) and (11) in part I[1]] were developed.

$$\frac{\partial C_v}{\partial t} = R_v + D\nabla^2 C_v - \frac{C_v}{M}\frac{\partial M}{\partial t} \tag{8}$$

$$\frac{\partial C_n}{\partial t} = R_n - \frac{C_n}{M}\frac{\partial M}{\partial t} \tag{9}$$

where $C_v$ and $C_n$ are the concentrations of small volatile and nonvolatile species, respectively. In part I, methods for calculating the reaction, diffusion, and boundary conditions for the solid–gas interface were discussed.

For the CSTRs-in-series model of segregated continuous reactors, eqs. (8) and (9) are extended, and discretized as shown.

$$\frac{\partial C_{v,j,k}}{\partial t} = R_{v,j,k} + D\nabla^2 C_{v,j,k} + \left(F_{j,k-1\rightarrow k}C_{v,j,k-1} - \left(F_{\text{exit},j,k} + F_{j,k\rightarrow k+1} + \frac{\partial M_{j,k}}{\partial t}\right)C_{v,j,k}\right)/M_{j,k} \tag{10}$$

$$\frac{\partial C_{n,j,k}}{\partial t} = R_{n,j,k} + \left(F_{j,k-1\rightarrow k}C_{n,j,k-1} - \left(F_{\text{exit},j,k} + F_{j,k\rightarrow k+1} + \frac{\partial M_{j,k}}{\partial t}\right)C_{n,j,k}\right)/M_{j,k} \tag{11}$$

Figure 7 summarizes the structure described above for a CSTRs-in-series model with four radial collocation points and four residence time stages. In Figure 7, each flow convects material of the originating element (a flow from element 1,1 to 1,2 will have the concentration of element 1,1). This means that, to apply eqs. (10) and (11), the various flows shown in Figure 7 must be calculated.

In part I, the average concentration of various species over a particle radius was calculated as

$$C_{v \text{ or } n,\text{avg}} = \int_0^1 C_{v \text{ or } n} x^{a-1}\, dx = \sum_j W_j C_{v \text{ or } n,j} \tag{12}$$

Examination of eq. (12) shows that $W_j$ can be interpreted as the mass fraction at collocation point $j$, because the concentrations have units of mol/kg. This means that the entering flows into the first stage should be apportioned according to $W_j$.

$$F_{\text{in},j} = W_j F_{\text{in,total}} \tag{13}$$

where

$$F_{\text{in,total}} = \sum_j F_{\text{in},j}$$

## Single Segregated CSTR

To model a single segregated CSTR, we can choose the number of stages to give the desired approximation to perfect segregation and the flows to give the single CSTR residence time distribution. The selection of residence times of eq. (5), $\Delta\tau_k$, was carried out by assigning values for each stage ($\tau_k$) according to the zeroes of an orthogonal polynomial formed from the basis set of $\{\exp(-\tau/\bar{\tau}), \tau\exp(-\tau/\bar{\tau})\cdots\}$. This has the quality of spacing the $\tau_k$ over the residence time distribution defined by $\bar{\tau}$. The time then to go from $\tau_{k-1}$ to $\tau_k$ is just $\Delta\tau_k$. To insure the residence time distribution for a CSTR, we must have the flow proportional to mass at each stage. Thus, the flow rate from one stage to the next is given by

$$F_{j,k-1\rightarrow k} = \frac{M_{j,k-1}}{\Delta\tau_k} \tag{14}$$

Notice that eq. (14) is consistent with eq. (7). Furthermore, eq. (7) showed the flow rate from each individual element must be proportional to the mass of that element. Determining the total exit flow ($F_{\text{out}}$) to regulate overall mass in the reactor, the exit flow rates are easily calculated as

$$F_{\text{exit},j,k} = \left(\frac{M_{j,k}}{\Sigma_{l,m} M_{l,m}}\right)F_{\text{out}} \tag{15}$$

Here, $j$ denotes the radial collocation point number and $k$ the residence time stage number.

The flows of Figure 7 are now completely defined; so, that the flow terms of eqs. (10) and (11) can be easily calculated with eqs. (13), (14), and (15), providing a simulation of a single segregated CSTR.

### Tubular Reactor

The reactor configuration above is convenient for modeling a single-stage stirred bed reactor; however, the common industrial configuration is that of Figure 1 (a tubular reactor). This section will discuss the how the flows of Figure 7 must be calculated to model a tubular reactor.

As discussed above, the tubular reactor will be modeled as CSTRs-in-series shown in Figure 6. Thus, there are no side draws, and only the outflow at the reactor end is allowed. Equation 13 for the inlet flow into the first stage remains unchanged.

The stages are allocated slightly differently than the single segregated CSTR case. Now, each stage is assumed to have the same mass. In other words, the stages are spaced evenly along the tubular reactor, and a mass balance dictates that

$$F_{j,k-1\rightarrow k} = F_{j,k\rightarrow k+1} \tag{16}$$

The model of part I assumes no change in particle size or density on loss of mass due to diffusion. This means that the relative mass at each collocation point is approximated as constant for purposes of diffusion calculations; so, eq. (16) makes the same assumption for calculating convective mass transport in the reactor. In addition, a particle of PET polymerizing from 15,000 to 30,000 g/mol will only lose 0.2% of its mass; thus, eq. (16) is justified.

Lastly, the exit flows from the final stage are calculated through a slightly modified version of eq. (15).

$$F_{j,k\rightarrow k+1|k=\text{final element}} = F_{\text{exit},j,k|k=\text{final element}} = \left(\frac{M_{j,k}}{\Sigma_l M_{l,k}}\right)\Bigg|_{k=\text{final element}} F_{\text{out}} \tag{17}$$

The flow equations for a tubular reactor are now specified. The additional terms of eqs. (10) and (11) can be easily calculated with eqs. (13), (16), and (17) and a tubular reactor simulated by the CSTRs-in-series model. The degree of axial dispersion introduced by this model can be found by relating a reactor Peclet number to the number of stages:

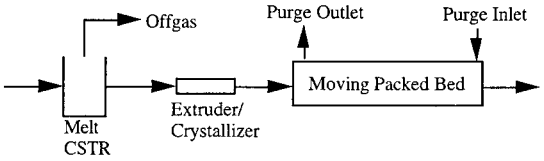


**Figure 8** Flowsheet for case study (PET).

$$Pe = \frac{uL}{D_L} = 2(\#\text{ of stages}) \tag{18}$$

### Reactor Gas Phase

In the case where the rate of mass transfer is calculated based on a concentration gradient, the gas phase concentrations are necessary. The gas phase is assumed to be isobaric and at constant volume. By assuming the ideal gas law, the only mol changes in the gas phase are based on temperature changes. Equations (19), (20), and (21) describe the reactor gas phase.

$$\frac{dy_{i,k}}{dt} = \left(F_{\text{in},k,\text{gas}}y_{i,k,\text{in}} - F_{\text{out},k,\text{gas}}y_{i,k} + \text{R}_{MT,i,k} - y_{i,k}\frac{dn_k}{dt}\right)/n_k \tag{19}$$

$$\frac{dn_k}{dt} = F_{\text{in},k,\text{gas}} - F_{\text{out},k,\text{gas}} \tag{20}$$

$$F_{\text{out},k,\text{gas}} = F_{\text{in},k,\text{gas}} + \frac{PV}{RT^2}\frac{dT_k}{dt} \tag{21}$$

Here, $y_{i,k}$ is the gas phase mol fraction of component $i$, $n_k$ is the number of mol in the gas phase at stage $k$, and $R_{\text{MT},i,k}$ is the rate of mass transfer to the gas phase of component $i$.

For a segregated CSTR, the particle are segregated, but the gas phase is well mixed so stages are unnecessary for the gas phase (the subscript $k$ is dropped). The inlet flows and concentrations are just those coming into the reactor. For both a segregated CSTR and tubular reactor each element is well mixed and intraparticle gradients do not need to be considered.

For the tubular reactor, the gas flows countercurrent to the polymer flow.

$$F_{\text{in},k,\text{gas}}y_{i,k,\text{in}} = F_{\text{out},k+1,\text{gas}}y_{i,k+1} \tag{22}$$

**Table II Operating Conditions for Example Reactor Train**

| | Finishing Reactor | Solid-State Reactor |
|---|---|---|
| Temperature | 300°C | 220°C |
| Residence time | 7500 s (~ 2 h) | 73000 s (~ 20 h) |
| Polymer feed | PET with $M_n$ = 9600<br>$\frac{1}{4}$ of endgroups carboxyl<br>feed rate = 144 kg/h | (Outlet from extruder) |
| Gas phase | 5 Torr | Purge $N_2$ rate: 612 kg/h<br>Purge has 20 ppm ethylene glycol and 20 ppm water<br>Atmospheric pressure |
| Mass transfer coeff. | 0.0017 mol/s/Torr | 0.04 mol/s/Torr (finite condensate concentration at solid–gas interface) |
| Reactor particles | — | 0.133 cm |
| Resid. time stages | | 10 (Peclet number = 20) |
| Polymer kinetics | Ravindranath et al.[11] (Table III) | |
| Water vapor pressure | $VP_{water} = 10^{\left(8.519 - \frac{2100}{T}\right)}$ | |
| Ethylene glycol vapor pressure | $VP_{ethylene\ glycol} = 10^{\left(9.396 - \frac{3070}{T}\right)}$ | |
| Polymer thermodyn. | Flory–Huggins with all chi values set to 0.5 | |

At the final stage, the inlet values are those of the feed gas.

## Energy Balance

The temperature at each reactor zone is calculated easily with an energy balance.

$$\frac{dT_k}{dt} = \Big( F_{\text{in},k,\text{gas}} C_{p,\text{in},k,\text{gas}} T_{\text{in},k,\text{gas}} + F_{\text{in},k,\text{poly}} C_{p,\text{in},k,\text{poly}} T_{\text{in},k,\text{poly}} - F_{\text{out},k,\text{gas}} C_{p,k,\text{gas}} T_k - F_{\text{out},k,\text{poly}} C_{p,k,\text{poly}} T_k + H_{\text{react},k} + H_{\text{cryst},k} + H_{\text{vap},k} + U_j (T_{\text{jacket}} - T_k) + E_T - C_{p,k} T_k \frac{dM_k}{dt} \Big) / (C_{p,k} M_k) \quad (23)$$

$$M_k = \sum_j M_{jk} \quad (24)$$

Here, $H_{\text{react},k}$, $H_{\text{cryst},k}$, and $H_{\text{vap},k}$ are the respective enthalpies of reaction, crystallization, and vaporization at stage $k$. $E_T$ is included for generality to represent volumetric heating, for example, dielectric heating. Also, the gas and particle temperatures are assumed to be the same at each stage.

For the segregated CSTR, the well-mixed assumption and the assumption of no intraparticle temperature gradients means that the $k$ subscript is unnecessary, the reactor is at a uniform temperature. For the tubular reactor, the purge gas flows from $k + 1$ to $k$, countercurrent to the polymer which flows from $k - 1$ to $k$. Each temperature zone is assumed to be well mixed, but the individual zones differ in temperature.

**Table III Converted PET Kinetic Constants of Ravindranath et al.[11]**

| Reaction (see Fig. 9) | Polycondensation | Acetaldehyde Formation | Esterification | Diester Group Degradation | Polycondensation of Vinyl End Group |
|---|---|---|---|---|---|
| Activation energy kcal/mol | 18.5 | 29.8 | 17.6 | 37.8 | 18.5 |
| Frequency factor kg/mol/h[a] | $9.91 \times 10^7$ | $5.0 \times 10^9$ | $1.52 \times 10^8$ | $2.2 \times 10^{11}$ | $9.91 \times 10^7$ |
| Equilibrium constant | 0.5 | — | 1.25 | — | — |

[a] Acetaldehyde formation and diester group degradation are unimolecular with units of $h^{-1}$.

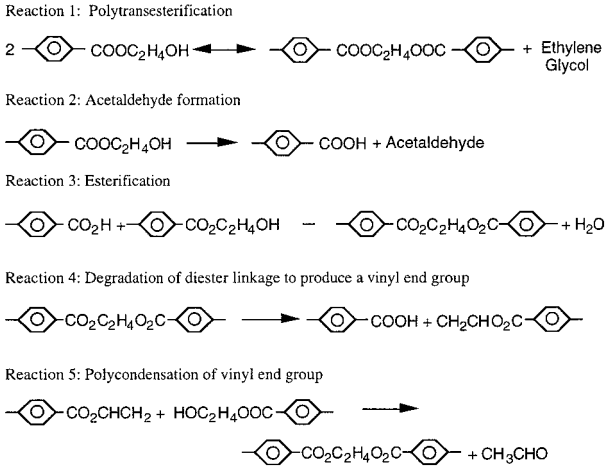


**Figure 9** Reaction mechanisms for PET (simplified from Ravindranath et al.[11]).

## A CASE STUDY OF A MOVING PACKED BED REACTOR

In this section, an example flowsheet (Fig. 8) is used to investigate the effect of various design parameters. To represent the final section of a process for producing PET, a finishing reactor (melt polymerization) will be connected to an extruder that then leads to a moving packed bed reactor (solid state reaction). The extruder connecting the two units is modeled with no holdup or reaction; the unit merely converts the melt to solid pellets. Table II shows the operating conditions for the finisher (modeled as a CSTR) and the solid-state reactor (assumed isothermal). Other particle scale parameters are listed in Table IV. The kinetic scheme is described in Table III and Figure 9.

In the figures that follow, the acetaldehyde, carboxyl end, and hydroxyl end content will not be shown explicitly; however, the model includes all these species. More detail on these reactions can be found in the first paper of this series[1] as well as the thesis of Mallon.[10] Changes in the carboxyl/hydroxyl ratio can be inferred from figures showing water and ethylene glycol in the polymer because these species control the equilibrium limited reaction.

A series of cases with changes from the base case solid-state reactor operation above will be studied (Figs. 10–16) to demonstrate and understand the parameter sensitivity: increasing the purge gas flow rate by 20%, increasing the solid-state reactor temperature by 5°C, and increasing the purge gas inlet concentrations to 120 ppm ethylene glycol and 1200 ppm water. In this case study, degree of polymerization refers to the number of monomers in the chain (number average). To convert to molecular weight multiply by 96 (the average monomer molecular weight without end groups).

Figure 10 shows the degree of polymerization profiles in the melt and solid-state reactors. Increasing the purge gas rate in the solid state reactor has very little effect. Temperature greatly increases the reaction rate (as expected). Finally, an increased condensate level in the purge gas feed stream reduces the reaction rate and causes the rate of polymerization to decrease toward the end of the reactor as condensate levels reach equilibrium. The effect of the energy balance will be shown later.

Continued reaction in the solid state is not the sole reason for the profiles in Figure 10. Because the purge gas flows counter to the polymer flow (Fig. 1), the gas phase condensate concentration and, consequently, the concentration in the polymer increase from the bottom of the reactor to the top. Equation (1) then finds that low levels of condensate lead to higher degrees of polymeriza-

**Table IV Parameters for PET Simulation**

| Parameter | Value | Source |
|---|---|---|
| Crystallizing rate | $3.6517 \times 10^{-14}\ \exp(23186/RT)$ | Mallon and Ray[1] |
| Maximum crystallinity | 0.390 + 0.0025 (T-470) | Mallon and Ray[1] |
| Diffusivity (water and ethylene glycol, $cm^2/s$) | $1.932 \times 10^{-6}\exp\left(\frac{-29670}{R}\left(\frac{1}{T}-\frac{1}{493}\right)\right)$ | Mallon Ray[1] |
| Radial colloc, points number | 4 | Adequate from preliminary simul. |
| Particle shape | Sphere | Assumption |
| Initial crystallinity | 0.30 | Assumption |

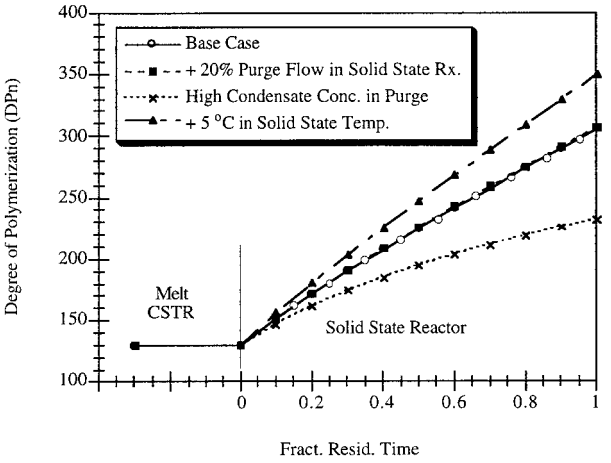


**Figure 10** Degree of polymerization in a moving packed bed reactor.

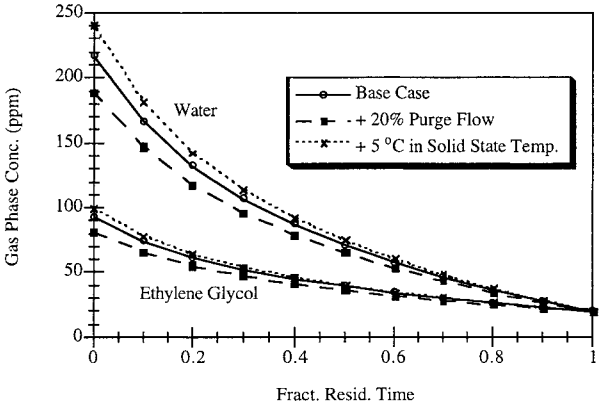


**Figure 12** Gas phase concentrations in a moving packed bed reactor.

tion. Figures 11–14 show the concentrations of water and ethylene glycol in the solid and gas phases (the high condensate concentration case is shown on separate figures to avoid confusion). The early peak in Figures 11 and 13 is a result of crystallization upon pelletization, which increases the amorphous phase concentration of reactive end groups, thus increasing the equilibrium extent of reaction without the need to remove more condensate.

The gas phase variations are also interesting. The effect of increased gas flow rate seems merely to dilute the condensate concentration. Increased temperature leads to increased mass transport rates, which causes higher gas phase concentrations and higher rates of polymerization. For high purge gas concentrations, concentration changes from the inlet to the exit are small.

We noted earlier that ethylene glycol in the purge gas suppresses the molecular weight profiles inside the polymer particles. Figures 15 and 16 show the effect of different purge gas compositions on degree of polymerization profiles inside the PET particles. Four cases were studied: 120 ppm ethylene glycol (and 1200 ppm water) at the gas inlet, 20 ppm ethylene glycol and water at the gas inlet, 5 ppm ethylene glycol and water at the gas inlet, and a high purge rate that forces gas phase concentrations to zero throughout the reactor (with the other parameters specified in Table II). The two figures represent two locations along the reactor (at the middle and the end); significant variation in the degree of polymerization is evident at both locations. Clearly, if one wants to suppress the profiles further, the condensate level in the purge gas should be raised. Figures 15 and 16 also show that the polymerization has proceeded mainly in a boundary layer close to the surface. Because increases in purge gas composi-

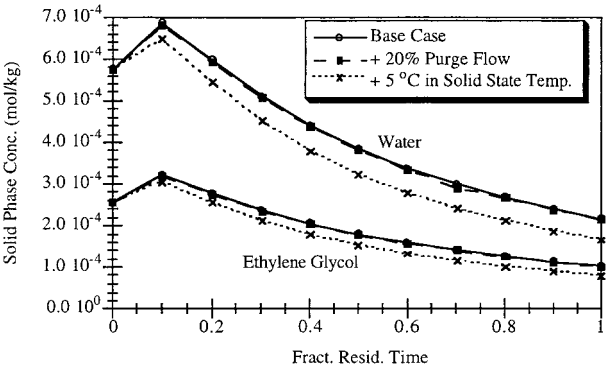


**Figure 11** Solid-phase volatile concentrations in a moving packed bed reactor.

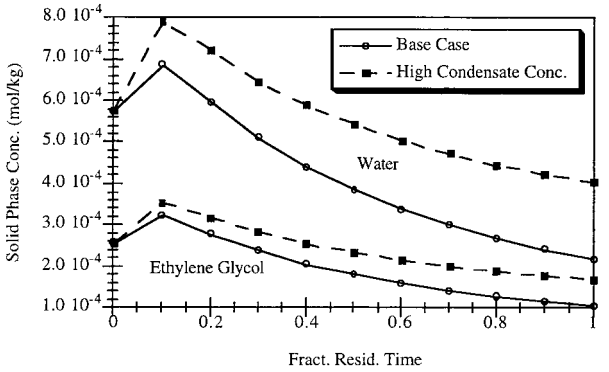


**Figure 13** Effect of high purge gas concentrations on solid phase in a moving packed bed reactor.

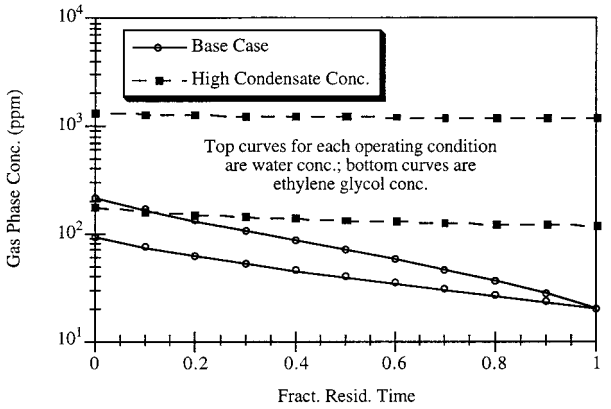


**Figure 14** Effect of high purge gas concentrations in gas phase in a moving packed bed reactor.

tion will depress conversion at the surface, the temperature must be raised or residence time increased to conserve overall conversion in the reactor.

Figures 15 and 16 also lend an understanding to the result of Yau and Cherry.[4] If decreased purge gas concentrations increase the variation in the molecular weight inside a particle, then the observed "gel" may just be very high molecular weight polymer at the particle edge. High molecular weights have long relaxation times and might be considered gel if the forming step is too fast.

### Energy Balance in a Solid-State Reactor

There are several situations that may cause the reactor to be nonisothermal. In this section, the energy balance for a PET solid-state reactor will be considered. Extra heating or heat transfer to the reactor wall is assumed to be negligible, and the heat of reaction for PET is essentially zero

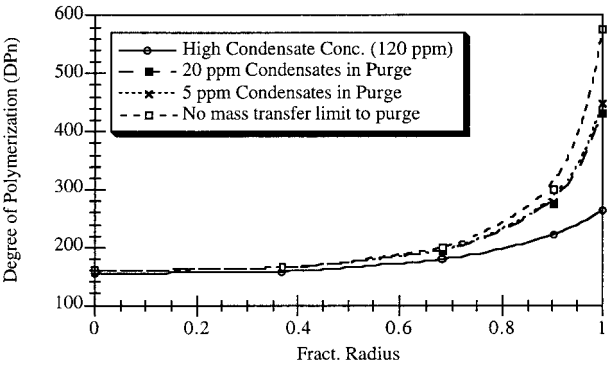


**Figure 15** Radial profiles in particles in the middle of a moving packed bed reactor.

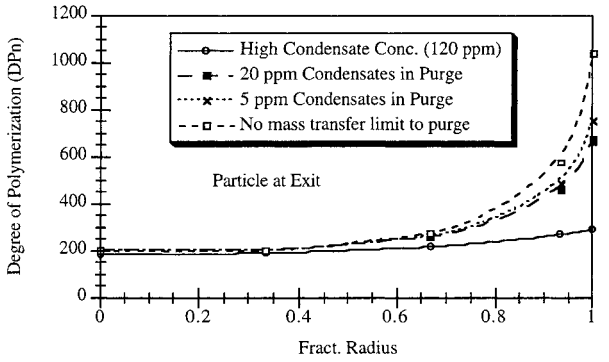


**Figure 16** Radial profiles in particles exiting a moving packed bed reactor.

from the kinetic scheme of Ravindranath et al.[11] The other contributions (due to inlet flows, condensate vaporization, and crystallization) will be calculated explicitly.

The heat up of the entering particle to reactor temperature occurs very close to the surface ($R^2/\alpha$ is about 10 s). Temperature profiles can then be determined by macroscopic energy transport with the microscopic behavior assumed to be fast. Therefore, the temperature profile can then be calculated by the CSTRs-in-series model.

Figures 17 and 18 show simulations with the same parameters as before except that the isothermal assumption is relaxed (parameters in Table V). Figure 17 shows the variation in bed temperature with several different assumptions; the stream temperature has the biggest effect on the energy balance. The heat of vaporization of condensate is the next most important effect with the heat of crystallization causing only a small change. Figure 18 shows that including the en-

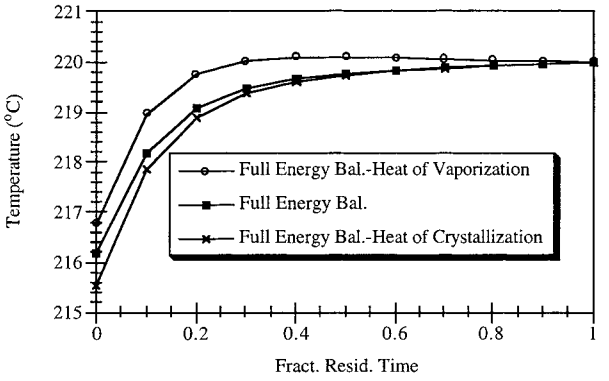


**Figure 17** Temperature distribution in a moving packed bed. Polymer entrance temperature dominates nonisothermal character.

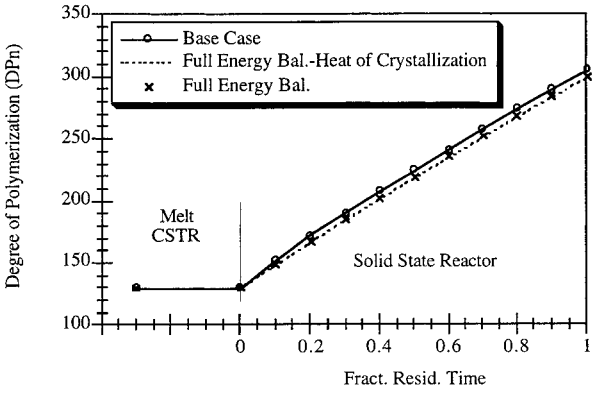


**Figure 18** Effect of including energy balance on reaction rate. Heat of crystallization has little effect.

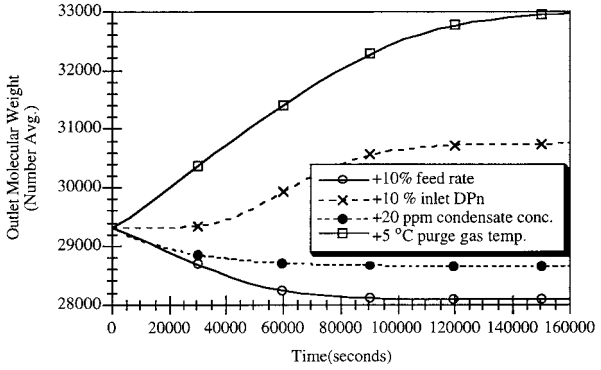


**Figure 19** Dynamic response of outlet molecular weight to step changes in possible control variables.

ergy balance has only a small effect on the degree of polymerization profiles in the reactor. Furthermore, the heat of crystallization causes no meaningful change in the reactor profiles.

The shape of the profile in Figure 17 depends on more than just the dispersion. As the purge gas flow is increased, the gradient at the boundary of the bed will become steeper, i.e., the heat capacity of the purge will dominate the heat capacity of the entering polymer. Quantitatively, the product of the gas flow rate and its heat capacity must be larger than the corresponding quantities for the polymer. Otherwise, the gas heat capacity will not dominate, and most of the bed will be at the entering polymer temperature and not the gas.

Some example simulations can illustrate additional effects. Two different cases are shown: one that shows the effect of different reactor Peclet numbers and inlet purge gas concentrations (Table VI) and one where the outlet molecular weight is held approximately constant (for Peclet number equal to 20) by varying the reactor residence times (Table VII). Both cases show that, when the purge gas condensate concentration is kept very low, the Peclet number for the particles in the reactor affects the final molecular weight more. However, with higher purge gas concentrations, longer residence times are required and the Peclet number has a small effect on molecular weight.

**Table V Parameters for Energy Balance Calculations**

| | |
|---|---|
| Inlet polymer temperature | 210°C |
| Inlet purge gas temperature | 220°C |
| Heat capacity of polymer | 437.3 cal/kg/°C |
| Heat capacity of water (Gaseous values used for atmos. pressure at 500 K, inconsequential in any case) | 474 cal/kg/°C |
| Heat capacity of nitrogen | 252.4 cal/kg/°C |
| Heat of vaporization of ethylene glycol | 11849 cal/mol |
| Heat of vaporization of water (taken from $H_v$, water from nylon 6[12]) | 18300 cal/mol |
| Heat of crystallization | 4687 cal/kg |

## Solid-State Reactor Dynamics

The dynamic behavior of a solid-state reactor can also be predicted from our model. An understanding of the dynamics of a solid-state reactor is important for reactor control. Figure 19 shows how the outlet degree of polymerization is affected by changes in reactor control variables: feed rate, feed DPn, gas concentration, and gas temperature. [The purge gas flow rate was not used due to the small effect seen earlier (Fig. 10).] The purge gas temperature curve is based on the full energy balance.

The change in molecular weight in response to a change of the inlet degree of polymerization displays a significant time delay. The dead time is of the order of the residence time of the reactor. Consequently, this variable is undesirable as a control variable. The particle feed rate has a slow response and is probably difficult to manipulate because it influences production targets and schedules. Because solid-state reactors are often run close to the sticking temperature to maximize the production, changing the purge gas is already constrained. In addition, due to the large thermal

**Table VI Effect of Peclet Number and Purge Gas on Outlet Molecular Weight**

| Conditions in Reactor | Pe = 20 | Pe = 40 |
|---|---|---|
| Molecular weight (number avg.) with ethylene glycol (120 ppm) and water (1200 ppm) in purge (mass transfer limit) | 22317 | 22563 |
| Molecular weight (number avg.) with ethylene glycol and water in purge (20 ppm) (mass transfer limit) | 29368 | 30016 |
| Molecular weight (number avg.) with ethylene glycol and water in purge (5 ppm) (mass transfer limit) | 29895 | 30588 |
| Molecular weight (number avg.) without ethylene glycol or water in purge (no mass transfer limit) | 31426 | 32112 |

mass of the reactor, the response to a purge gas temperature change takes a long time. This case study would then suggest that the purge gas condensate concentration is the best manipulated variable for controlling the reactor outlet molecular weight. This case study illustrates the usefulness of a dynamic model in the design of control systems for a solid state reactor.

### The Relative Importance of Heat and Mass Balances

The example particle and reactor system studied here has shown that condensate mass transfer has a much larger effect on the polymerization than the energy balance (Table VI). This relative importance is primarily caused by the proximity of ethylene glycol to its boiling point (197°C). As the temperature increases, the vapor pressure increases dramatically, increasing the driving force for mass transfer. For example, by increasing the temperature to 230°C from 220°C, the vapor pressure increases by about 30%. If the user then reduced nitrogen flow rates by 30%, the temperature gradient of Figure 17 would propagate further into the polymer bed; however, the energy input needed to vaporize the ethylene glycol would still be fairly minimal (about 0.5°C in bed temperature).

To see significant effects due to the heat required to vaporize ethylene glycol, the purge gas rate must be reduced significantly. However, to avoid mass transfer limitations, the purge gas concentrations must be low, requiring a significant purge gas flow rate. If one increased the reactor temperature to 230°C and reduced the flow rate of purge gas by a factor of 3, the heat of vaporization of ethylene glycol would cause the purge gas to cool by about 2°C from bottom to top. Still, this change in temperature will only cause about a 3% change in reaction rate. For other reactor designs the reactor model can be used to determine the relative importance of heat transfer vs. mass transfer.

## CONCLUSIONS

In this work, the relative merits of different reactor configurations were discussed with the principal focus on the moving packed bed reactor. Then, after developing a general model for solid-state reactors, a case study was carried out on a moving packed bed reactor to determine the relative im-

**Table VII Effect of Peclet Number on Outlet Molecular Weight**

| Conditions in Reactor | Pe = 20 | Pe = 40 | Relative Res. Time |
|---|---|---|---|
| Molecular weight (number avg.) with ethylene glycol (120 ppm) and water (1200 ppm) in purge | 28955 | 29023 | 10 |
| Molecular weight (number avg.) with ethylene glycol and water in purge (20 ppm) | 29368 | 30016 | 1.0 |
| Molecular weight (number avg.) with ethylene glycol and water in purge (5 ppm) | 29357 | 30016 | 0.96 |
| Molecular weight (number avg.) without ethylene glycol or water in purge (no mass transfer limit) | 29345 | 29917 | 0.86 |

pact of different parameters. Reactor temperature and purge gas concentration both affected the final degree of polymerization. To demonstrate the applicability of the model for process control, a series of dynamic simulations was performed to ascertain the dynamic behavior of the model. The effect of the energy balance, for the case study considered, was found to be small.

## REFERENCES


1. F. K. Mallon and W. H. Ray, *J. Appl. Polym. Sci.,* **69,** 1233 (1998).
2. K. Ravindranath and R. A. Mashelkar, *J. Appl. Polym. Sci.,* **39,** 1325 (1990).
3. J. Zimmerman, *J. Polym. Sci., Polym. Lett. Ed.,* **2,** 955 (1964).
4. C. C. Yau and C. Cherry, U.S. Pat. to Eastman Chemical #5,393,871 (1995).
5. L. J. Balint, R. L. Abos, and O. E. Snider, U.S. Pat. to Allied Chemical #3,544,525 (1970).
6. D. Herron, U.S. Pat. to Bepex Corp. #4,161,578 (1979).
7. H. Rüssemeyer, M. Kerl, H. Schmidt, B. Häni, and W. Kägi, U.S. Pat. to Bühler #5,090,134 (1992).
8. M. Caracotsios, *ISCRE,* **12,** 1992.
9. T. N. Zwietering, *Chem. Eng. Sci.,* **11,** 1 (1959).
10. F. K. Mallon, PhD Thesis, Univ. of Wisc. Madison (1997).
11. K. Ravindranath and R. A. Mashelkar, *AIChE J.,* **30,** 415 (1984).
12. O. Fukumoto, *J. Polym. Sci.,* **22,** 263 (1956).